Sea surface temperature variability in the Pacific sector of the Southern Ocean over the past 700 kyr

Sze Ling Ho,[1] Gesine Mollenhauer,[1] Frank Lamy,[1] Alfredo Martínez-Garcia,[2] Mahyar Mohtadi,[3] Rainer Gersonde,[1] Dierk Hebbeln,[3] Samuel Nunez-Ricardo,[4,5] Antoni Rosell-Melé,[6,7] and Ralf Tiedemann[1]

Received 12 March 2012; revised 10 September 2012; accepted 11 September 2012; published 12 October 2012.

[1] In spite of the important role played by the Southern Ocean in global climate, the few existing paleoceanographic records in the east Pacific sector do not extend beyond one glacial-interglacial cycle, hindering circumpolar comparison of past sea surface temperature (SST) evolution in the Southern Ocean. Here we present three alkenone-based Pleistocene SST records from the subantarctic and subtropical Pacific. We use a regional core top calibration data set to constrain the choice of calibrations for paleo SST estimation. Our core top data confirm that the alkenone-based U^{K}_{37} and $U^{K'}_{37}$ values correlate linearly with the SST, in a similar fashion as the most commonly used laboratory culture-based calibrations even at low temperatures (down to ~1°C), rendering these calibrations appropriate for application in the subantarctic Pacific. However, these alkenone indices yield diverging temporal trends in the Pleistocene SST records. On the basis of the better agreement with $\delta^{18}O$ records and other SST records in the subantarctic Southern Ocean, we propose that the U^{K}_{37} is a better index for SST reconstruction in this region than the more commonly used $U^{K'}_{37}$ index. The U^{K}_{37}-derived SST records suggest glacial cooling of ~8°C and ~4°C in the subantarctic and subtropical Pacific, respectively. Such extent of subantarctic glacial cooling is comparable to that in other sectors of the Southern Ocean, indicating a uniform circumpolar cooling during the Pleistocene. Furthermore, our SST records also imply massive equatorward migrations of the Antarctic Circumpolar Current (ACC) frontal systems and an enhanced transport of ACC water to lower latitudes during glacials by the Peru-Chile Current.

Citation: Ho, S. L., G. Mollenhauer, F. Lamy, A. Martínez-Garcia, M. Mohtadi, R. Gersonde, D. Hebbeln, S. Nunez-Ricardo, A. Rosell-Melé, and R. Tiedemann (2012), Sea surface temperature variability in the Pacific sector of the Southern Ocean over the past 700 kyr, *Paleoceanography*, *27*, PA4202, doi:10.1029/2012PA002317.

1. Introduction

[2] The Southern Ocean plays a key role in global climate via its influence in the meridional overturning circulation [*Marshall and Speer*, 2012] and the global carbon cycle [*Fischer et al.*, 2010]. Knowledge of past changes in this ocean is therefore essential for a better understanding of its mechanistic link to the global climate and ultimately contributes to improving the prediction of future climate change via modeling efforts. In this regard, sea surface temperature (SST), as the interface between the ocean and the atmosphere, is an indispensable boundary parameter in driving global climate models. Our present understanding of Pleistocene SST evolution in the Southern Ocean is mostly derived from sediment records in the Atlantic sector [*Martínez-Garcia et al.*, 2009; *Schneider-Mor et al.*, 2008], the Indian sector [*Howard and Prell*, 1992], and the Southwest Pacific [*Pahnke et al.*, 2003; *Schaefer et al.*, 2005]. The eastern Pacific sector of the Southern Ocean, on the other hand, is a less studied region. The few existing high-resolution marine archives spanning one glacial cycle off Chile at ODP Site 1233 (41°S) indicate a dramatic equatorward shift (7–10°) of the Southern Ocean current systems [*Verleye and Louwye*, 2010] and substantial glacial cooling of 5 to 7°C based on a coccolithophorid transfer function and alkenones [*Kaiser et al.*, 2005; *Lamy et al.*, 2004;

[1]Alfred Wegener Institute for Polar and Marine Research, Bremerhaven, Germany.
[2]Geological Institute, ETH Zürich, Zurich, Switzerland.
[3]MARUM-Center for Marine Environmental Sciences, University of Bremen, Bremen, Germany.
[4]Department of Zoology, Facultad de Ciencias Naturales y Oceanográficas, Universidad de Concepción, Concepción, Chile.
[5]Now at Programa de Biología, Facultad de Ciencias Básicas, Universidad del Magdalena, Santa Marta, Colombia.
[6]Institució Catalana de Recerca i Estudis Avançats, Barcelona, Spain.
[7]Also at Institut de Ciència i Tecnologia Ambientals, Universitat Autònoma de Barcelona, Bellatera, Spain.

Corresponding author: S. L. Ho, Alfred Wegener Institute for Polar and Marine Research, PO Box 12 01 61, DE-27515 Bremerhaven, Germany. (sze.ling.ho@awi.de)

0883-8305/12/2012PA002317

Saavedra-Pellitero et al., 2011]. Further south at 53°S, an alkenone-based SST record off the Strait of Magellan [*Caniupán et al.*, 2011] displays glacial cooling of up to ~8°C. Meanwhile, a time-slice study of the LGM at the East Pacific Rise using a foraminiferal transfer function indicates a smaller amplitude of glacial-interglacial SST changes of 2 to 5°C between 48°S and 57°S [*Luz*, 1977]. The few South Pacific data in a circumpolar compilation from the subantarctic and the Antarctic zones of the Southern Ocean based on siliceous microfossil records [*Gersonde et al.*, 2005] suggest less severe glacial cooling (~1.5°C) in the Pacific compared to the other sectors during the Last Glacial Maximum (LGM). Notably, all these records do not extend beyond the last two glacial-interglacial cycles, hindering the comparison of temperature evolution in different sectors of the Southern Ocean and Antarctica on orbital timescales. The lack of paleo SST records in the subantarctic Pacific also precludes the examination of the SST gradients between low and high latitudes, from which the latitudinal migration of the oceanic frontal systems and the advection of the vigorous eastern boundary current, i.e., the Peru-Chile Current (PCC), could be inferred. The transport of subantarctic cold water by the PCC to the tropics could influence the SST in the cold tongue especially during glacial periods, as demonstrated by foraminiferal census data and a simple heat model [*Feldberg and Mix*, 2002, 2003].

[3] For the evaluation of the SST gradient, it would be ideal if the individual SST records were derived from the same proxy and calibration in order to minimize the discrepancy that might arise from dissimilar habitat depth and/or sensitivity of biological proxies to environmental changes. In this work, we employ the most commonly applied organic geochemical SST proxy, i.e., the alkenone paleothermometry. It is based on the relative distribution of di-, tri- and tetra-unsaturated long-chain alkenones consisting of 37 carbon atoms, generally known as $C_{37:2}$, $C_{37:3}$, and $C_{37:4}$, respectively. The degree of alkenone unsaturation is a function of growth temperature of the precursor, i.e., haptophyte algae. An index known as U^{K}_{37} (=[$C_{37:2}$ − $C_{37:4}$]/[$C_{37:2}$ + $C_{37:3}$ + $C_{37:4}$]) has been proposed to quantify the degree of unsaturation [*Brassell et al.*, 1986], and it was later simplified to $U^{K'}_{37}$ (=[$C_{37:2}$]/[$C_{37:2}$ + $C_{37:3}$]) since the $C_{37:4}$ alkenones are often absent in open ocean sediments where overlaying SSTs are higher than 12°C [*Prahl and Wakeham*, 1987]. Over the years, work has been mainly focused on the simplified $U^{K'}_{37}$ index, which is applicable to most parts of the global ocean. However, alkenone-derived glacial SSTs that are warmer than those of the interglacial have been observed in the Sea of Okhotsk [*Harada et al.*, 2006] and the northeast Atlantic [*de Vernal et al.*, 2006; *Rosell-Melé and Comes*, 1999], raising doubts about the applicability of alkenone paleothermometry at high latitudes. Another potential caveat, i.e., the nonlinearity of the relationship of $U^{K'}_{37}$ index and SST at low temperatures (<6°C), has also been suggested [*Conte et al.*, 2006; *Rosell-Melé*, 1998; *Rosell-Melé et al.*, 1994; *Sikes and Volkman*, 1993]. It is still debatable whether U^{K}_{37} or $U^{K'}_{37}$ is the more appropriate SST proxy at high latitudes due to the lack of data in this region, especially in the Southern Ocean.

[4] In this study we revisit the alkenone paleothermometry at the lower end of the temperature range and assess the applicability of the alkenone indices by using regional surface sediments. We present three SST records to investigate the temporal pattern and the amplitude of the paleo SST evolution in the South Pacific along the latitudinal range of the PCC spanning both subtropical and subantarctic oceanic zones. On the basis of our SST reconstruction, we infer the latitudinal migration of the oceanic fronts and discuss their paleoclimatic implications.

2. Oceanographic Setting

[5] The Peru-Chile Current (PCC; also known as Peru Current, Chile-Peru Current, and Humboldt Current) and the Antarctic Circumpolar Current (ACC) are the main features of the surface circulation in the Southeast Pacific (Figure 1). The eastward flowing ACC is driven by the intense midlatitude Southern Hemisphere westerly winds (Westerlies). Thus its latitudinal migration is closely related to the wind-forcing [*Orsi et al.*, 1995]. The circumpolar transport of the ACC is approximately 107 Sv, with most of the transport occurring in the Subantarctic Front (SAF) and the Antarctic Polar Front (APF) [*Cunningham et al.*, 2003]. The impingement of the northern part of the ACC onto the South American continent leads to a bifurcation around 43°S, yielding a vigorous equatorward branch (PCC) and a weaker poleward branch (Cape Horn Current, CHC) [*Strub et al.*, 1998]. The PCC flows northward along South America and is deflected away from the coast at around 5°S, feeding the cold PCC water into the South Equatorial Current which flows westward as the equatorial cold tongue between 10°S and 4°N [*Wyrtki*, 1965]. Meanwhile, the CHC moves along the coastal region of southernmost Chile, mixing the subantarctic water with low salinity regional water and transporting this modified ACC water to the Atlantic Ocean via the Drake Passage [*Chaigneau and Pizarro*, 2005]. The Westerlies shift northward in the winter as a result of seasonal fluctuations of sea ice around Antarctica [*Kidston et al.*, 2011]. Modern day austral winter is also marked by more vigorous advection of cold water toward the tropics and a larger temperature gradient between low and high latitudes.

[6] Our South Pacific core top sites are located between the Subtropical Front (STF) and the APF, where the modern day annual mean temperatures of the overlaying surface waters are in the range of ~1 to ~12°C. Our long piston core sites are well suited for studying the open ocean PCC, as they are beyond the direct influence of the intense coastal upwelling that is confined within 50–60 km of the shoreline [*Strub et al.*, 1998]. Sites GeoB 3327–5 and PS75/034–2 are located at the northern extent of the ACC, in sensitive regions where the latitudinal movement of the ACC is expected to be registered. The southernmost site PS75/034–2 is located ~7° and ~9° north of the modern day mean location of the SAF and the APF, respectively. Site GeoB 3388–1 lies within the flowpath of the PCC, thus the SST changes here reflect the extent of the cold water advection by the PCC.

3. Materials and Methods

3.1. Materials

[7] We analyzed 34 core top samples (Figure 1) recovered by multicorer from the Pacific sector of the Southern Ocean between the STF and the APF, but alkenones were detected at only 13 sites (see Table 1 for coordinates). Two piston

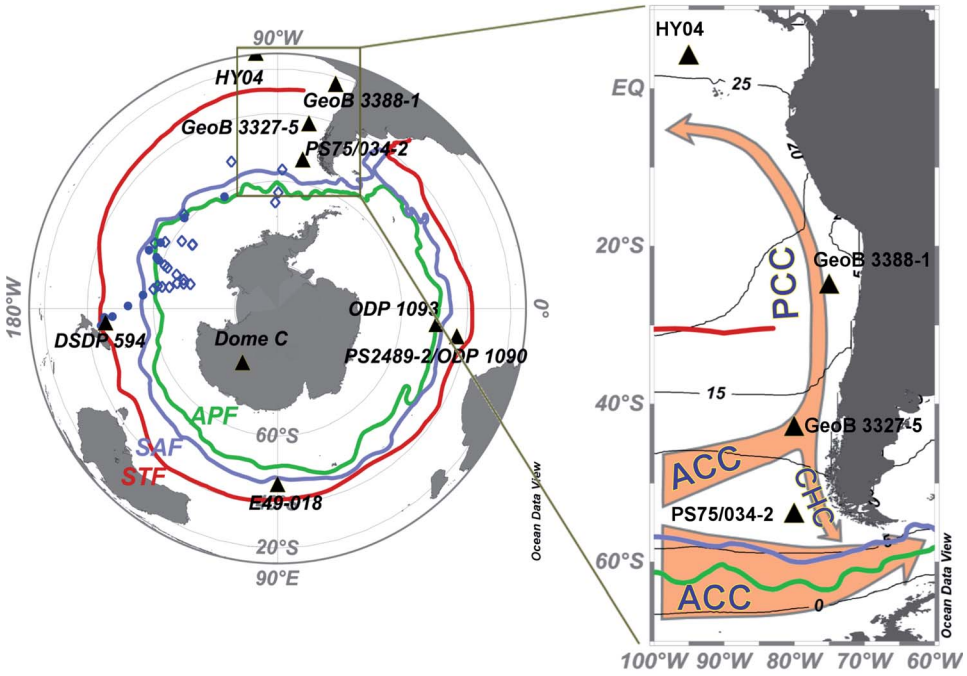

Figure 1. Location of sites and major oceanic currents discussed in this work. For the purpose of this study, the subantarctic region is defined as the waters between the Subtropical Front and the Subantarctic Front. Blue circles denote the sites of the core top data in the regional alkenone unsaturation calibration, while blue open diamonds denote the sites where alkenones were below detection limit. Black triangles denote the sites of SST records used for discussion. In addition to the newly presented records (GeoB 3388–1, GeoB 3327–5, and PS75/034–2), we also include several previously published SST records from the tropics (HY04 [*Horikawa et al.*, 2010]) and the Southern Ocean (DSDP 594 [*Schaefer et al.*, 2005], E47–018 [*Howard and Prell*, 1992], PS2489-ODP Site 1090 [*Martínez-Garcia et al.*, 2009] and ODP Site 1093 [*Schneider-Mor et al.*, 2008]), in addition to the Antarctic temperature record at EPICA Dome C [*Jouzel et al.*, 2007]. Thin black lines indicate the annual mean isotherms in degree Celsius (°C) derived from the World Ocean Atlas 2009 (WOA09). Orange arrows indicate major surface currents, and colored lines illustrate the oceanic frontal system [after *Orsi et al.*, 1995]. Abbreviations: APF = Antarctic Polar Front; SAF = Subantarctic Front; STF = Subtropical Front; PCC = Peru-Chile Current; ACC = Antarctic Circumpolar Current; CHC = Cape Horn Current.

cores in the subantarctic Pacific sector of the Southern Ocean and one piston core from the subtropical South Pacific were analyzed in this study (Figure 1). Core GeoB 3327–5 (43°14′S, 79°59′W, 3534 m water depth, 900 cm length) and core GeoB 3388–1 (25°13′S, 75°31′W, 3558 m water depth, 710 cm length) were retrieved during the R/V Sonne cruise 102 [*Hebbeln et al.*, 1995], while core PS75/034–2 (54°22′S, 80°05′W, 4425 m water depth, 1808 cm length) was collected during the Alfred Wegener Institute expedition ANT XXVI/2 with R/V Polarstern [*Gersonde et al.*, 2011]. The sediments of core GeoB 3327–5 alternate between clayey foraminifera and clayey foraminifera nannofossil ooze, while core GeoB 3388–1 consists of mainly nannofossil ooze. Core PS75/034–2, on the other hand, due to its location below the carbonate compensation depth, consists of mainly siliceous clay and is barren of foraminifera. The sampling intervals for core GeoB 3327–5 and GeoB 3388–1 were 5 cm throughout the core. Core PS75/034–2 was sampled every 10 cm throughout the core and every 5 cm in the section between 200 cm and 310 cm.

3.2. The δ^{18}O Measurement on Foraminifera

[8] A Finnigan MAT 251 mass spectrometer coupled with a Kiel device inlet system was used to measure the δ^{18}O composition of planktic *Neogloboquadrina pachyderma* (dextral coiling) from the >150 μm size-fraction and benthic *Cibicides spp.* from the >212 μm size-fraction for core GeoB 3327–5. The measurements were performed on approximately 5–10 individual tests. For all stable isotope measurements a working standard was used, which was calibrated against VPDB (Vienna Pee Dee Belemnite) by using the NBS 19 standard. Consequently, all isotopic data are relative to the PDB standard. Long-term analytical standard deviation is ±0.07 ‰ (Isotope Laboratory, Faculty of Geosciences, University of Bremen).

3.3. Alkenone Analysis

[9] Sample preparation and alkenone analysis of cores GeoB 3327–5 and GeoB 3388–1 were carried out according to the procedure described by *Müller et al.* [1998]. About 3–14 g of freeze-dried and ground sediment samples were

Table 1. Site Information and Alkenone Index Values of the Southern Ocean Core Top Samples Retrieved via Multicoring

Site	Longitude	Latitude	WOA09 Annual Mean SST (°C)	U^{K}_{37}	$U^{K'}_{37}$
PS75/034–1	80.09 °W	54.37°S	6.71	0.213	0.256
PS75/104–2	174.53 °E	44.77°S	11.74	0.371	0.411
PS75/099–1	177.27 °E	48.26°S	9.24	0.294	0.294
PS75/072–3	151.22 °W	57.56°S	1.89	0.007	0.086
PS75/082–2	158.36 °W	59.04°S	1.52	−0.012	0.081
PS75/098–6	179.01 °W	52.97°S	7.47	0.217	0.275
PS75/105–1	174.62 °E	44.41°S	11.74	0.486	0.486
PS75/095–6	174.43 °W	57.02°S	4.95	0.178	0.214
PS75/101–2	175.88 °E	45.81°S	11.12	0.296	0.324
PS75/080–2	157.64 °W	58.18°S	2.08	−0.021	0.084
PS75/053–1	115.98 °W	60.77°S	3.01	0.016	0.085
PS75/076–1	156.14 °W	55.53°S	4.68	0.089	0.219
PS75/063–2	135.62 °W	58.90°S	2.18	−0.007	0.093

subjected to three times of sonication in mixtures of methanol and dichloromethane with decreasing polarity. The supernatant was then rinsed with deionized water and sodium sulfate, before being concentrated and passed through a short bed of silica (Bond-Elut silica cartridge, Varian) to purify the fraction that contained the alkenones. The fraction was then saponified to remove esters. The quantification of alkenones was achieved using gas chromatography on an HP 5890, equipped with a 60 m fused silica capillary column (DB-5 MS, Agilent) and a flame ionization detector. The oven temperature was programmed to rise from 50 to 250°C at a rate of 25°C/min, then to 290°C at a rate of 1°C/min, followed by 26 min of isothermal period, before being ramped up to 310°C at a rate of 30°C/min and held constant for 10 min. Replicate analyses of laboratory internal reference sediment suggest analytical errors of ~0.5°C for both alkenone indices (U^{K}_{37} and $U^{K'}_{37}$).

[10] Piston core PS75/034–2 was analyzed at the Alfred Wegener Institute (Bremerhaven). The extraction of organic compounds was accomplished using a Dionex ASE-200 pressurized solvent extractor, with a mixture of methanol and dichloromethane in the ratio of 1:9. Similar to the treatment for the GeoB cores, the total extract was separated into 3 fractions via silica gel fractionation using hexane, DCM, and methanol, respectively. The fraction (eluted with DCM) containing the alkenones was then concentrated and analyzed by gas chromatography on an HP 6890 fitted with a flame ionization detector and a 60 m DB-1 MS column (Agilent). The initial temperature in the oven was set to 60°C. After the injection of samples, the temperature in the oven was ramped up to 150°C at a rate of 20°C/min, followed by a reduced rate of heating at 6°C/min until the final temperature of 320°C was achieved and held constant for 40 min. The alkenone fraction of this sediment core was pure enough for quantification without saponification. We did not observe any systematic differences in the alkenone index values between saponified and untreated extracts in the six samples we tested. They agreed within ±0.015 units and ±0.012 units for U^{K}_{37} and $U^{K'}_{37}$, respectively, corresponding to ±0.47°C and ±0.37°C using the culture calibrations of *Prahl et al.* [1988]. Reproducibility of the instrument is estimated to be 0.17°C based on replicate analysis of alaboratory *E. huxleyi* culture extract.

[11] South Pacific core top samples were subjected to microwave-assisted extraction, followed by compound class fractionation using a Thermo Surveyor HPLC system equipped with a Lichrosphere Silicon dioxide column, according to the methods described by *Fietz et al.* [2011]. The fraction containing alkenones (eluted with DCM) was saponified to remove coeluting esters, prior to analysis by gas chromatography (same GC system used for the alkenone analysis of piston core PS75/034–2 described above).

[12] The concentrations of sediment extracts were adjusted such that the amounts of alkenones injected for each measurement were above threshold values (>5–10 ng) to avoid unjust bias due to low concentrations. The threshold values were previously suggested by *Villanueva and Grimalt* [1996], *Rosell-Melé et al.* [1995] and *Sonzogni et al.* [1997].

3.4. Alkenone-Based Indices and Calibrations

[13] The identification of alkenones was achieved by comparing chromatographic retention times of the samples with those of standards. The alkenone-based index (U^{K}_{37} and $U^{K'}_{37}$) values were calculated according to the previously proposed equations given in section 1. In order to compare these two alkenone indices in downcore reconstructions and to compare SST records spanning the tropics and the subantarctic Pacific, we need U^{K}_{37} and $U^{K'}_{37}$ calibrations that are based on a common data set and covering the largest possible temperature range. For this purpose, we opted to convert the index values into sea surface temperature using the widely used *E. huxleyi* culture-based calibrations proposed by *Prahl et al.* [1988], i.e., $U^{K}_{37} = 0.04\ T - 0.104$ ($r^2 = 0.98$) and $U^{K'}_{37} = 0.034\ T + 0.039$ ($r^2 = 0.99$), the latter being statistically identical to those based on global core top compilations [*Conte et al.*, 2006; *Müller et al.*, 1998].

3.5. SST Gradient Calculation

[14] We calculated the SST gradient along the latitudinal range of the PCC using alkenone-derived SSTs. We preferred the U^{K}_{37} index over the commonly used simplified version that excludes the $C_{37:4}$ alkenone, i.e., $U^{K'}_{37}$ (see justification in section 5.2). Considering the complexity of the hydrography in the eastern equatorial Pacific (EEP), we selected an open-ocean site HY04 (4°02′N 95°03′W) [*Horikawa et al.*, 2010] that is beyond the influence of the east Pacific cold tongue and the Peru coastal upwelling to examine the equator-to-pole SST gradients. A recent core top calibration study of *Kienast et al.* [2012] suggests that

the alkenone unsaturation in the open ocean EEP conforms to the established global core top calibrations. For the sake of consistency in the comparison, we recalculated the $U^{K'}_{37}$-derived SST estimates at site HY04 using the laboratory culture-based calibration of *Prahl et al.* [1988], assuming that $C_{37:4}$ alkenones are absent here. This results in similar U^{K}_{37} and $U^{K'}_{37}$ values. The assumption is justified by the fact that $C_{37:4}$ alkenones are numerically significant at growth temperatures below 15°C [*Prahl et al.*, 1988] and that the difference between U^{K}_{37} and $U^{K'}_{37}$ is only significant at ~10°C [*Rosell-Melé*, 1998]. Indeed, the recalculated SST estimates based on the U^{K}_{37} index are within ±0.5°C of the original $U^{K'}_{37}$-derived SST record reported in the literature (Figure 6) with exactly the same temporal trends. The SST records were resampled every 2 kyr for the calculation of the gradients between sites.

4. Results

4.1. Stratigraphy

[15] In order to obtain a consistent stratigraphic framework for all records in the SST gradients calculation, we tuned all available benthic δ^{18}O records to the global benthic δ^{18}O stack LR04 [*Lisiecki and Raymo*, 2005] using the software package AnalySeries 2.0 [*Paillard et al.*, 1996]. For this purpose, we revised the published age model of GeoB 3388–1 [*Mohtadi et al.*, 2006] which was previously aligned to the orbitally tuned ODP Site 677 [*Shackleton et al.*, 1990]. Overall, the differences between the revised and the original age models are minimal, with one exception during the time interval between 400 kyr and 500 kyr, especially at the termination of MIS 12. The linear sedimentation rates (LSR) at site GeoB 3388–1 fluctuate between 2.2 and 0.3 cm kyr^{-1}, with an average of less than 1 cm kyr^{-1} over the past 700 kyr.

[16] The age model of core GeoB 3327–5 was similarly generated via graphical tuning of the *Cibicides spp.* benthic δ^{18}O record to the LR04 global benthic stack. According to the age model, the record extends back to 513 kyr and spans the past five glacial-interglacial cycles (Figure 3). Average sedimentation rate is 2.6 cm kyr^{-1} and the values range between 0.7 cm kyr^{-1} and 4.4 cm kyr^{-1} without any drastic fluctuation. The only exception is a brief interval during MIS 7, where sedimentation rates reach about 10 cm kyr^{-1}, which may suggest redeposition. However, there is no lithological indication for, e.g., turbidites during this interval. A lack of chronological tie points for MIS 9 and part of MIS 8 arises as a result of poor carbonate preservation.

[17] In core PS75/034–2 carbonate preservation is poor, thus a benthic foraminifera-based δ^{18}O record could not be obtained. The attempt to use radiolarian biofluctuation for chronological control [*Hays et al.*, 1976] has also failed due to low abundance of *Cycladophora davisiana* (0–2.5% throughout the core) (G. Cortese, unpublished data, 2011). There are no well-dated marine records in the subantarctic Pacific that would provide a reference chronology for graphical tuning of the downcore oscillations in the physical properties (e.g., lightness, major elements, magnetic susceptibility). In the absence of other alternatives, we graphically tuned the PS75/034–2 U^{K}_{37} record to the temperature evolution registered in the EPICA ice core at Dome C, Antarctica [*Jouzel et al.*, 2007], based on the updated chronology EDC3 [*Parrenin et al.*, 2007]. Justification for the preference of the U^{K}_{37} index over the $U^{K'}_{37}$ index is outlined in section 5.2. The EPICA ΔT record was adjusted by a 15-point moving average smoothing prior to the graphical alignment to accommodate the much lower temporal resolution in core PS75/034–2. Our EDC3-derived age model is supported by the shipboard biostratigraphy based on diatom zonation (*Thalassiosira lentiginosa*) [*Zielinski and Gersonde*, 2002], i.e., ~178 kyr and ~350 kyr in our EDC3-based chronology correspond to the boundaries of MIS 6/7 and 9/10 as indicated by the biostratigraphy. The fairly uniform linear sedimentation rate throughout the core (1.4–3.5 cm kyr^{-1}) (Figure 2) and the resemblance in the general patterns between core PS75/034–2 and other Southern Ocean records (Figure 5) provide additional confidence in the stratigraphic framework. We adopted the original age model of core HY04 [*Horikawa et al.*, 2010], which is based on visual alignment of the benthic foraminiferal δ^{18}O to the orbitally tuned ODP Site 677 [*Shackleton et al.*, 1990] for the upper 420 kyr, and the lower part of the record to the LR04 global stack. There is no significant temporal offset between the upper 420 kyr of this δ^{18}O record (on current time scale) and the LR04 benthic stack.

4.2. South Pacific Core Top Alkenone Calibrations

[18] As shown in Figure 3, both U^{K}_{37} and $U^{K'}_{37}$ indices correlate linearly to annual mean WOA09 SST (with r^2 values of 0.94 and 0.93, respectively) for the temperature range of 1.5 to 11.7°C. These regressions are identical within estimation error to the extrapolated *Prahl et al.* [1988] calibrations below 8°C.

4.3. Downcore SST Estimates and Planktic δ^{18}O Values

4.3.1. Core GeoB 3388–1

[19] At subtropical site GeoB 3388–1, the $U^{K'}_{37}$-derived SSTs for the past 700 kyr range between 15°C and 21°C (Figure 4a). The index suggests that SST during MIS 12 is slightly colder (~2°C) than the average glacial SST, while MIS 13 is the coolest interglacial. Meanwhile, the U^{K}_{37}-inferred SSTs at site GeoB 3388–1 are in the range of 16°C to 22°C. The amplitudes of glacial/interglacial SST variations in both U^{K}_{37}- and $U^{K'}_{37}$-derived records are ~6°C.

4.3.2. Core GeoB 3327–5

[20] The $U^{K'}_{37}$-SST estimates are between ~5°C and ~14°C over the past 513 kyr at site GeoB 3327–5 (Figure 4c). While there is not much difference in the warmth of interglacials, the $U^{K'}_{37}$-inferred estimates suggest strong variability in the severity of glacials, with SSTs from ~5°C during MIS 10 to ~10°C during MIS 6. On the other hand, the U^{K}_{37}-derived glacial-interglacial SST oscillations at site GeoB 3327–5 range between ~8°C and ~16°C, without any substantial long-term trend in glacial cooling and interglacial warming. Alkenones in the top of a multicore at this site register U^{K}_{37}- and $U^{K'}_{37}$-inferred SST estimates of 15.4°C and 13.9°C, respectively.

[21] The δ^{18}O values of planktic dextral-coiling *N. pachyderma* range between 1.1 to 3.1‰ (Figure 4b). There is a data gap between MIS 8 and MIS 10 because of carbonate dissolution. The δ^{18}O values during MIS 11 are more enriched than those in other interglacials. Some abrupt shifts toward more depleted values are recorded during MIS 11 and 12.

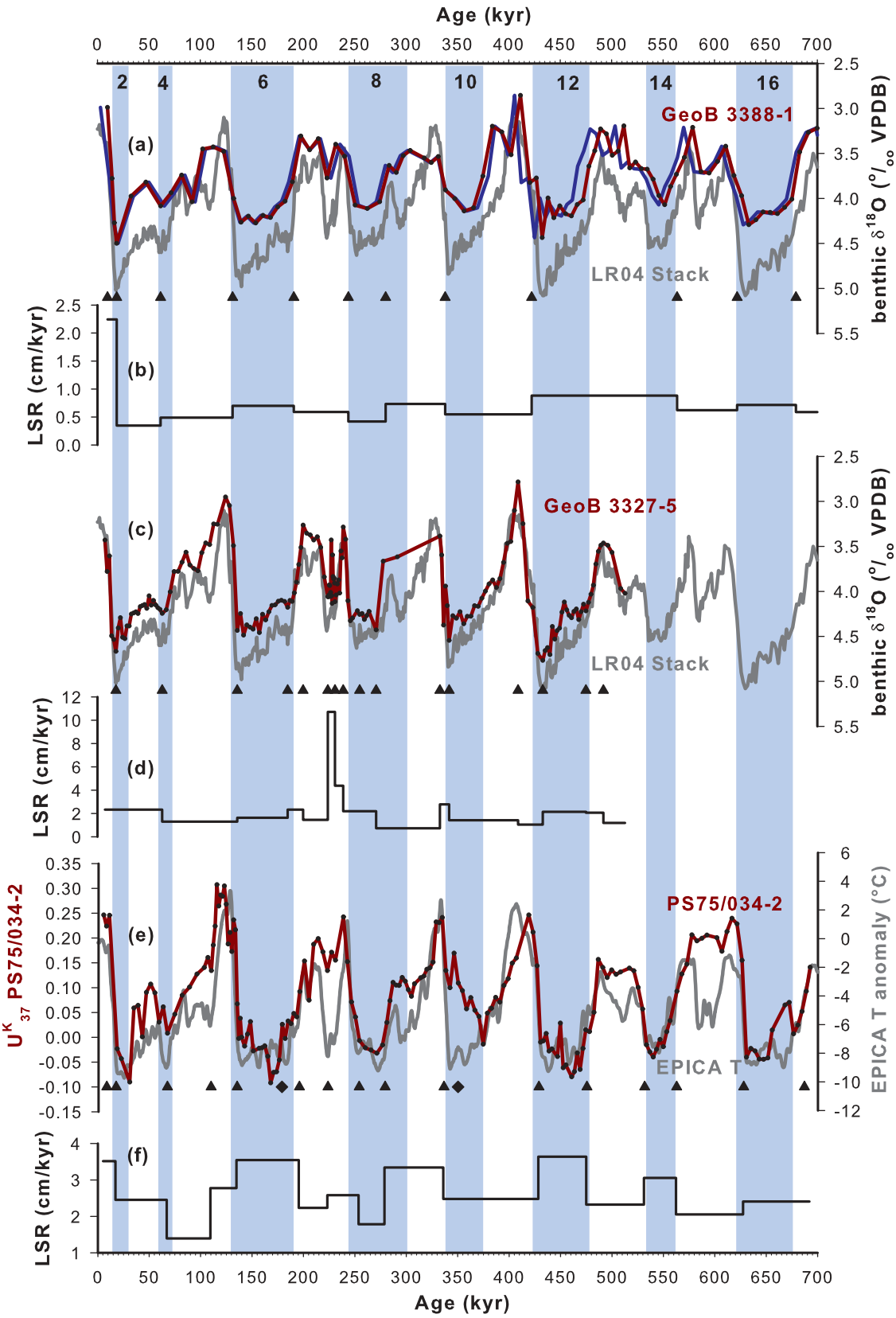
Age (kyr)
0 50 100 150 200 250 300 350 400 450 500 550 600 650 700
2 4 6 8 10 12 14 16
(a)
GeoB 3388-1
LR04 Stack
benthic δ18O (°/oo VPDB)
2.5 3.0 3.5 4.0 4.5 5.0 5.5
(b)
LSR (cm/kyr)
2.5 2.0 1.5 1.0 0.5 0.0
(c)
GeoB 3327-5
LR04 Stack
benthic δ18O (°/oo VPDB)
2.5 3.0 3.5 4.0 4.5 5.0 5.5
(d)
LSR (cm/kyr)
12 10 8 6 4 2 0
(e)
PS75/034-2
EPICA T
U^K37 PS75/034-2
0.35 0.30 0.25 0.20 0.15 0.10 0.05 0.00 -0.05 -0.10 -0.15
EPICA T anomaly (°C)
6 4 2 0 -2 -4 -6 -8 -10 -12
(f)
LSR (cm/kyr)
4 3 2 1
0 50 100 150 200 250 300 350 400 450 500 550 600 650 700
Age (kyr)

Figure 2

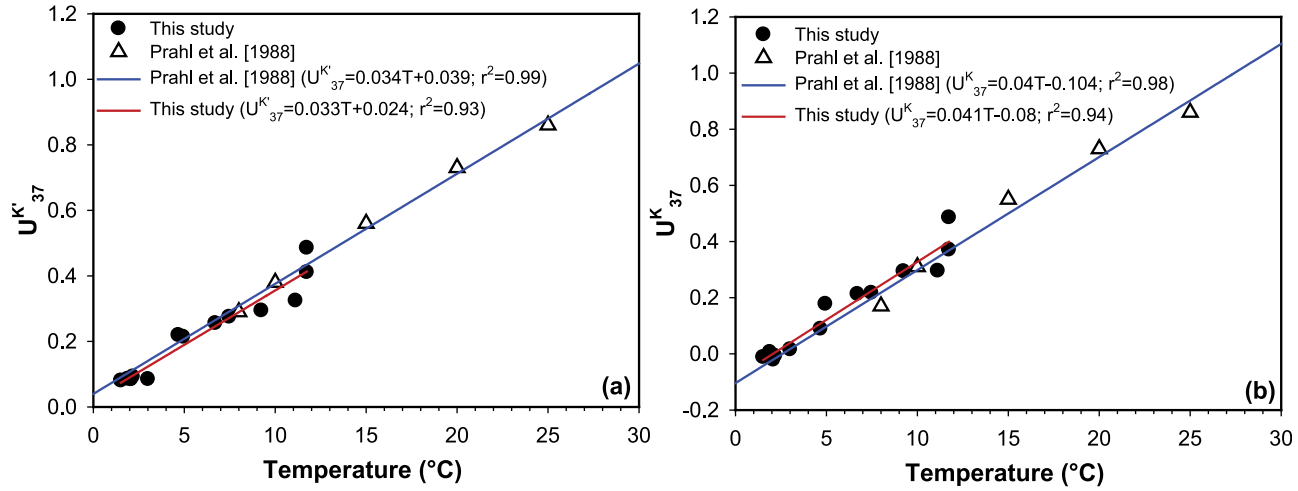

Figure 3. Correlations of alkenone indices (a) $U^{K'}_{37}$ and (b) U^{K}_{37} with temperature. The sediment core top data were calibrated against the WOA09 annual mean SST, while the *E. huxleyi* culture data of *Prahl et al.* [1988] plotted against the growth temperature as reported in the original publication. Blue line illustrates the linear regressions proposed by *Prahl et al.* [1988], with extrapolation for temperatures below 8°C. Red line denotes our South Pacific core top calibration (through the black circles).

4.3.3. Core PS75/034–2

[22] The overall SST variability suggested by the $U^{K'}_{37}$ index at site PS75/034–2 is between ~1°C and ~8°C, resulting in a glacial-interglacial amplitude of up to ~7°C (Figure 4d). The $U^{K'}_{37}$ index indicates that MIS 10 is the coldest glacial, while MIS 5 is the warmest interglacial. During the interval between MIS 16 and MIS 12, the $U^{K'}_{37}$-inferred glacial-interglacial cycles are not pronounced due to substantially smaller amplitude of SST oscillations (~2°C compared to ~7°C after MIS 12). The $U^{K'}_{37}$-derived SST estimates for these glacial intervals (especially MIS 16) are as warm as the SST estimates for the subsequent interglacial intervals. The $U^{K'}_{37}$ index suggests a pervasive long-term trend in the glacial cooling, i.e., the glacial SSTs decrease from MIS 16 to MIS 10, and increase thereafter to MIS 6, followed by a colder MIS 2. On the other hand, the U^{K}_{37}-derived SSTs at site PS75/034–2 range between ~1°C and ~10°C over the past 700 kyr (Figure 4d). According to the U^{K}_{37}-derived SST estimates, the severity of glacial SSTs does not vary substantially at site PS75/034–2. MIS 10 is slightly warmer (~2°C) than the other glacial periods, while MIS 5 and MIS 13 stand out as the warmest and coolest interglacials, respectively. The SST estimates inferred from the $U^{K'}_{37}$ and the U^{K}_{37} indices for the top of a multicore at this site are 6.4°C and 7.9°C, respectively.

5. Discussion

5.1. Alkenone-Based Calibrations for Application in the Subantarctic Pacific

[23] Here we use the *E. huxleyi* culture-based alkenone calibrations from *Prahl et al.* [1988] for SST reconstruction. While the $U^{K'}_{37}$-SST relationship of this calibration has been confirmed by global core top calibrations [*Conte et al.*, 2006; *Müller et al.*, 1998] with extensive data sets encompassing diverse biogeographic provinces and a wide temperature range, the U^{K}_{37}-SST correlation has not been calibrated globally. Thus the U^{K}_{37}-SST relationship outside the calibration range (T < 8°C) is unknown except for the North Atlantic and the Nordic Sea [*Bendle and Rosell-Melé*, 2004; *Bendle et al.*, 2005; *Rosell-Melé et al.*, 1994; *Rosell-Melé et al.*, 1995]. Considering the low modern SST at our southern site PS75/034–2 (WOA09 annual mean SST of 6.7°C), the paleo SST here, especially during glacials,

Figure 2. Age models and linear sedimentation rates at core sites GeoB 3388–1, GeoB 3327–5, and PS75/034–2. Shaded bars indicate glacial intervals, and the black numbers in the bars represent the marine isotope stages. Black triangles illustrate the stratigraphic tie points while the black diamonds mark the shipboard biostratigraphic points based on diatom zonation. (a) Stratigraphic framework for core GeoB 3388–1 was revised by graphical tuning of the benthic foraminiferal δ^{18}O record (red curve) to the benthic δ^{18}O stack LR04 (gray curve) [*Lisiecki and Raymo*, 2005]. The previously published age model [*Mohtadi et al.*, 2006] is represented by the blue curve. (b) Linear sedimentation rate at site GeoB 3388–1 derived using the stratigraphic tie points based on the benthic δ^{18}O record. (c) Stratigraphic framework for core GeoB 3327–5 was established by graphical tuning of the benthic foraminiferal (*Cibicides spp.*) δ^{18}O record (red curve) to the benthic δ^{18}O stack LR04 (gray curve) [*Lisiecki and Raymo*, 2005]. (d) Linear sedimentation rate at site GeoB 3327–5 based on the tuned benthic δ^{18}O record. (e) Stratigraphic framework for core PS75/034–2 was established by graphical tuning of the U^{K}_{37} record (red curve) to the smoothed (15-points running average) EPICA ΔT record at Dome C, Antarctica [*Jouzel et al.*, 2007; *Parrenin et al.*, 2007] (gray curve). (f) Linear sedimentation rate at site PS75/034–2 based on tuning to the EPICA ΔT record.

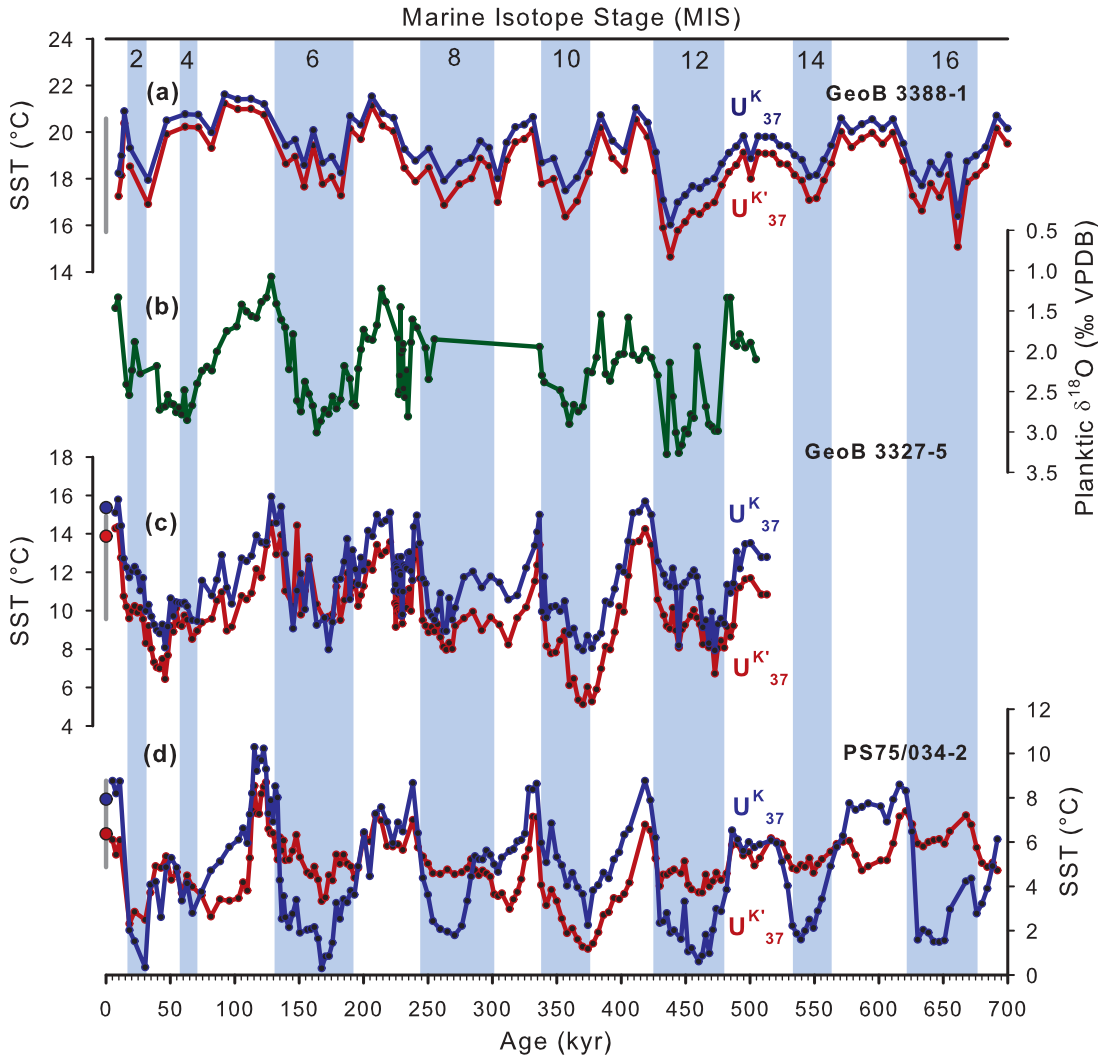

Figure 4. Planktic $\delta^{18}O$ and alkenone-based SST records. Shaded bars indicate glacial intervals and the black numbers in the bars represent the marine isotope stages. Gray bars denote modern day maximum and minimum SSTs derived from WOA09. (a) SST records derived from alkenone based indices, i.e., U^{K}_{37} (blue) and $U^{K'}_{37}$ (red) at site GeoB 3388–1. (b) Planktic $\delta^{18}O$ of dextral-coiling *N. pachyderma* at site GeoB 3327–5. Poor carbonate preservation result in a data gap from MIS 8 to MIS 9. (c) SST records derived from alkenone based indices, i.e., U^{K}_{37} (blue) and $U^{K'}_{37}$ (red) at site GeoB 3327–5. Filled circles indicate core top data at the same site. (d) SST records derived from alkenone based indices, i.e., U^{K}_{37} (blue) and $U^{K'}_{37}$ (red) at site PS75/034–2. Filled circles indicate core top data at the same site.

are likely to be well below the calibrated temperature range of the culture calibration (8–25°C). To better constrain our choice of calibrations, we examine the alkenone index values in the South Pacific surface sediments and find that first, the linearity of both U^{K}_{37}- and $U^{K'}_{37}$-SST correlations holds even at low temperatures in the South Pacific, indicating that both indices faithfully record modern SSTs in this temperature range. Second, the sedimentary alkenone unsaturation-SST relationships in the South Pacific are comparable to those observed in the *E. huxleyi* culture of *Prahl et al.* [1988], rendering these culture calibrations suitable for application in this region. Indeed, the U^{K}_{37} and the $U^{K'}_{37}$ calibrations resulted in core top SST estimates (8°C and 6°C at PS75/034–2; 15°C and 14°C at GeoB 3327–5) that are within the range of modern seasonal SSTs (see gray bars in Figure 4; 5°–9°C at PS75/034–2 and 10°–15°C at GeoB 3327–5). We refrain from using our own core top calibrations for down-core reconstruction because of their limited calibration range (~1°–12°C) which makes them inappropriate for the application in the subtropics for calculating the meridional SST gradients.

[24] We note that our finding is in contrast to that of the Southern Ocean core top calibration study of *Sikes et al.* [1997]. The better correlation in the $U^{K'}_{37}$-SST relationship (r^2 value of 0.92 compared to r^2 value of 0.76 for U^{K}_{37}-SST) led the authors to suggest that the $U^{K'}_{37}$ is the better index for paleo SST reconstruction in the Southern Ocean. Application of their calibrations at our sites yields core top SST estimates (U^{K}_{37} and $U^{K'}_{37}$: 14°C and 9°C at PS75/034–2; 21°C and 16°C at GeoB 3327–5) that are warmer than those inferred from the *Prahl et al.* [1988] calibrations. The warm bias is especially pronounced in the U^{K}_{37}-derived estimates,

which are substantially warmer than the modern day warmest month SST in WOA09 (see gray bars in Figure 4; ~9°C at PS75/034–2; ~15°C at GeoB 3327–5). These anomalously warm estimates produced by the core top calibrations of *Sikes et al.* [1997], in addition to a good match between our South Pacific core top calibrations and the *Prahl et al.* [1988] culture calibrations, led us to choose the latter calibrations to estimate paleo SSTs at our study sites in the subantarctic Pacific.

5.2. Assessing Contrasting Temporal Trends in U^{K}_{37}- and $U^{K'}_{37}$-Derived SST Records

[25] In alkenone-based SST records, the temporal trend is governed by the definition of the index, while the amplitude of downcore variation and the absolute value are determined by the calibration employed. In the subtropics (GeoB 3388–1), the SST patterns inferred from both U^{K}_{37} and $U^{K'}_{37}$ indices are similar, and their values are in agreement within 1.5°C. As discussed in section 5.1, the strong linear relationship between both the U^{K}_{37} and the $U^{K'}_{37}$ indices in the subantarctic surface sediments with the overlaying SSTs (i.e., comparable r^2 values) imply that both indices may be used to obtain paleo SST estimates in the region (Figure 3). However, downcore reconstructions yield a different picture, i.e., the indices result in contrasting subantarctic SST patterns for cores GeoB 3327–5 and PS75/034–2 (Figure 4). For the past two glacial-interglacial cycles, the $U^{K'}_{37}$–derived SSTs display a so-called Type 1 [*Schneider et al.*, 1999] alkenone SST record which is typical for the tropics and the monsoon-influenced region, characterized by a relatively warm MIS 6 and the occurrence of the coldest glacial SST in the middle or the inception of glacials. There is also a warming trend of glacials from MIS 10 to MIS 6 in these subantarctic $U^{K'}_{37}$ records. On the other hand, the U^{K}_{37}-derived SST records suggest little fluctuation in the severity of glacial intervals and the MIS 6 is as cold as other glacial intervals (a Type 3 alkenone SST record according to the definition of *Schneider et al.* [1999]), which shows more resemblance to the global ice volume oscillations documented in the benthic $\delta^{18}O$ record. The differences in temporal trends are especially clear for the time interval MIS 16 – 12 at our southernmost site PS75/034–2, during which the $U^{K'}_{37}$-derived SSTs exhibit a reduced amplitude of glacial-interglacial SST variations due to relatively warm glacials, especially MIS 16 which is as warm as interglacial MIS 11. However, the U^{K}_{37} index record suggests that the glacial SSTs during this time interval are consistent with those from other glacial intervals. Interestingly, such observations are not limited to the South Pacific. As shown in Figure 5c, dissimilar amplitudes of glacial-interglacial SST oscillations during MIS 12–16 are also evident in the alkenone-derived SST records at PS2489–2/ODP Site 1090 in the midlatitudes of the South Atlantic [*Martínez-Garcia et al.*, 2010; *Martínez-Garcia et al.*, 2009], suggesting that this divergene can be found throughout the Southern Ocean south of the Subtropical Front. To determine which pattern is more realistic, we further compare our alkenone records with the planktic $\delta^{18}O$ record at the same site, and with other subantarctic SST records from other sectors of the Southern Ocean (Figure 5). Since the most outstanding divergence in the two different alkenone SST patterns is in the long-term trend of the glacial severity (interglacial warmth is consistent), we focus our discussion on the cold intervals.

[26] Contrary to the $U^{K'}_{37}$–based SST records, the planktic $\delta^{18}O$ records in the South Pacific (GeoB 3327–5) and the South Atlantic (PS2489–2 / ODP Site 1090) [see *Venz and Hodell*, 2002] suggest minor oscillations in glacial severity. Apart from global ice volume and SST, the planktic $\delta^{18}O$ records are also influenced by changes in sea surface salinity (SSS). However, given the lack of any major freshwater sources in the vicinity of sites GeoB 3327–5 and PS2489–2/ODP Site 1090, large perturbations to the SSS at these sites over the past 700 kyr are unlikely. SSS here might be driven by an enhanced influence of low SST and low SSS polar water mass during glacials. However, in such a scenario, the SSS variations would be accompanied by concurrent changes in SST. Therefore we believe that SSS variations are not the reason for the diverging trends between the planktic $\delta^{18}O$ and the $U^{K'}_{37}$ records.

[27] In addition to a warming trend in glacial severity from MIS 10 to MIS 6, the $U^{K'}_{37}$ SST estimates for MIS 12, 14, and 16 are relatively warm at sites PS75/034–2 and PS2489/ODP Site 1090, even though MIS 12 and MIS 16 are known to be among the most severe glacial stages during the Pleistocene [*Lang and Wolff*, 2011; *Shackleton*, 1987]. We note that varying Pleistocene glacial severity is not physically impossible. Indeed, a SST record in the subtropical Agulhas region suggested its occurrence [*Bard and Rickaby*, 2009]. Here, MIS 10 and 12 are substantially colder than other glacials in the past 800 kyr but the glacial-interglacial cycles before MIS 12 are well-defined, unlike in the subantarctic $U^{K'}_{37}$ records. Furthermore, the Agulhas core site is located north of the Subtropical Front, under the influence of a completely different hydrographic setting (e.g., warm Agulhas current and associated eddies) from that of the subantarctic Southern Ocean. These differences suggest that the varying glacial severity trends in *Bard and Rickaby*'s [2009] Agulhas SST record and the subantarctic $U^{K'}_{37}$ SST records are unrelated.

[28] On the other hand, the glacial severity trends in U^{K}_{37}-derived SST records are in agreement with the planktic $\delta^{18}O$ records at site GeoB 3327–5 and PS2489–2/ODP Site 1090. At the latter site, a summer SST record inferred from foraminiferal assemblages further supports this pattern [*Becquey and Gersonde*, 2002, 2003] (Figure 5d). Similar patterns in glacial severity over the past 700 kyr has been observed elsewhere in the subantarctic Southern Ocean and Antarctica, such as ODP Site 1093 and ODP Site 1094 in the South Atlantic [*Schneider-Mor et al.*, 2008], DSDP Site 594 off New Zealand [*Schaefer et al.*, 2005], South Indian [*Howard and Prell*, 1992], and Antarctic atmospheric temperature records at EPICA Dome C [*Jouzel et al.*, 2007] and Dome Vostok [*Petit et al.*, 1999] (Figures 5e–5h). These temperature records suggest that unvarying glacial severity is a pervasive Pleistocene climatic feature in the Southern Ocean.

[29] The better agreement of the temporal trend of the U^{K}_{37} than the $U^{K'}_{37}$ SST records with other surface proxy records in the same oceanic region suggests that the U^{K}_{37}-derived SSTs are plausibly more realistic than the $U^{K'}_{37}$ estimates at these sites, even though the core top values of both indices correlate equally well with modern SSTs. Our findings agree with a multiproxy comparison study off the Iberian margin [*Bard*, 2001]. The author found that the U^{K}_{37}-derived glacial coolings were more comparable with those derived from other

proxies, even though the core top SST estimates inferred from both U^{K}_{37} and $U^{K'}_{37}$ indices were comparable with the observed annual average SST. These findings demonstrate that different alkenone indices could result in diverging paleo SST patterns during the cold intervals even if the core top SST estimates suggested by both indices agree with the modern day SST. The discrepancy in paleo SST patterns stems from the higher relative abundance of the $C_{37:4}$ alkenones during the cold intervals. Having established that the U^{K}_{37} index is a more suitable SST proxy in the subantarctic Pacific (south of the Subtropical Front at ~30°S), we base our stratigraphic framework of PS75/034–2 and the following discussion on the SST variations and the meridional gradients on the U^{K}_{37}- derived SST records.

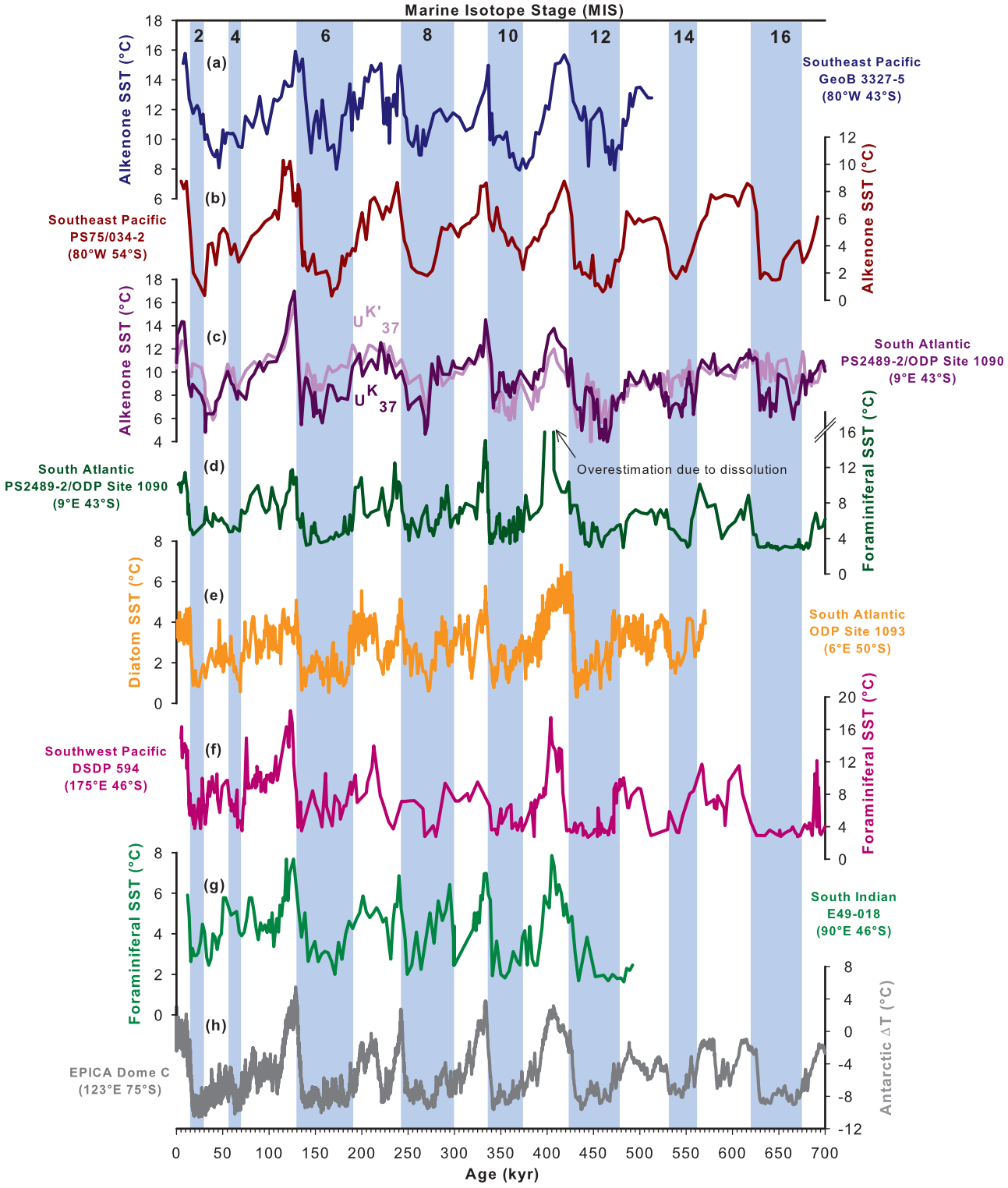

Figure 5

5.3. Southern Ocean SST Evolution: Circum-Antarctic Comparison

[30] High-resolution alkenone SST records off Chile (e.g., ODP Site 1233 and MD07–3128) suggest that the SST in the midlatitude Southeast Pacific evolved in synchrony with the atmospheric temperature at Antarctica on millennial timescales over the past 70 kyr [*Caniupán et al.*, 2011; *Kaiser et al.*, 2005; *Lamy et al.*, 2004]. Owing to the coarser temporal resolution in our Pleistocene SST records, it is impossible to assess these millennial-scale patterns. Instead, our SST records, especially the southern site, share first-order patterns on glacial-interglacial timescale with the EPICA Dome C temperature record of *Jouzel et al.* [2007]. There are, however, some minor differences compared to the Antarctic temperature record, such as the absence of a lukewarm interglacial MIS 15 at site PS75/034–2, and a cooling during MIS 3 at site GeoB 3327–5. Besides, unlike in the Antarctic temperature record, the Mid-Brunhes Event (∼430 kyr) shift is not well expressed in our SST records from the Southeast Pacific (Figure 5). This suggests an overprint of regional climate in our subantarctic SST records on the background of glacial-interglacial climatic changes closely linked to Antarctica. Meanwhile, other features such as the coolest MIS 13 and the warmest MIS 5 in the past 700 kyr, and the smallest amplitude of termination during the MIS 14–MIS 13 transition observed in our records are common in many marine and terrestrial records [*Lang and Wolff*, 2011]. With the exception of a warmer-than-today MIS 5 and a colder-than-today MIS13, the maximum SST estimates for other interglacials at sites GeoB 3327–5 and PS75/034–2 are similar to modern day summer SST (Figure 4).

[31] The intensity of Pleistocene glacial cooling (∼8°C) at our subantarctic Pacific sites is within the range of other subantarctic SST records derived from various proxies (Figure 5), i.e., ∼5°C in the South Indian [*Howard and Prell*, 1992], ∼7 to 10°C in the Southwest Pacific [*Pahnke et al.*, 2003; *Schaefer et al.*, 2005], and ∼7 to 11°C in the South Atlantic [*Becquey and Gersonde*, 2003; *Martínez-Garcia et al.*, 2009], indicating that the Pleistocene glacial cooling in the southeast Pacific is comparable, if not stronger, than in other sectors of the Southern Ocean. This is in contrast to the findings of *Gersonde et al.* [2005] in a circum-Antarctic LGM SST study using siliceous microfossil transfer functions. The authors reported a nonuniform glacial cooling in the Southern Ocean, with less cooling (∼1°C) in the Pacific compared to the Atlantic and Indian sectors (4–5°C). The discrepancy between this study and our compilation may be due to the more climatically sensitive sites of the long Pleistocene records (i.e., DSDP 594, GeoB 3327–5, PS75/034–2, MD97–2021). Alternatively, it could also be due to the different sensitivity of proxies (siliceous microfossils versus geochemical/carbonaceous microfossils) or the fact that the South Pacific is underrepresented in their calibration database. Indeed, foraminiferal assemblage-based LGM time slice studies suggest cooling of ∼5°C in the subantarctic Southeast Pacific (111°–123°W) [*Luz*, 1977] and up to ∼8°C in the Southwest Pacific [*Barrows and Juggins*, 2005], in better agreement with our alkenone-based estimates than those derived from the siliceous microfossil transfer functions.

[32] If true, the substantial Pleistocene glacial cooling in the subantarctic Southeast Pacific suggested by the alkenone paleothermometry is plausibly due to an extensive equatorward migration of the Westerlies and the Southern Ocean frontal systems embedded within the ACC, superimposed on the generally colder climate during glacials. Such equatorward shift of the oceanic systems might have occurred as a consequence of a massive northward sea ice expansion by 5° to 10°, as suggested previously by various faunal-based sea-ice and IRD records in the Southern Ocean [*Becquey and Gersonde*, 2002, 2003; *Crosta et al.*, 2004; *Gersonde et al.*, 2005]. By using the present as an analog for the past and assuming that the SST ranges associated with the oceanic fronts during glacial intervals would remain the same as modern day (∼5°C in the SAF and ∼2°C in the APF as in Figure 1), the average glacial SST estimates for sites PS75/034–2 (∼1°C) and GeoB 3327–5 (∼9°C) imply that both the SAF and the APF were located between 43°S and 54°S in the Southeast Pacific during glacials. This suggests that these oceanic fronts underwent substantial equatorward migration of ∼7° (SAF) and ∼9° (APF) during glacials and resided northward of site PS75/034–2. Such frontal migrations are conceivable, considering that no shallow bathymetric feature stands between site PS75/034–2 and the modern average latitudes of these oceanic fronts. Thus no topographic obstacle restricts the equatorward movement. In fact, frontal shifts (SAF and APF) of such magnitude during the Pleistocene have previously been proposed for the subantarctic Atlantic [*Becquey and Gersonde*, 2003] and the Southwest Pacific [*Schaefer et al.*, 2005; *Wells and Okada*, 1997].

[33] Such massive equatorward shifts of the ACC and its associated fronts in the Southeast Pacific may have important implications for the water transport through the Drake Passage. If, for instance, the SAF and the APF, which transport the bulk of the water in the ACC system, would be

Figure 5. Comparison of temperature records from the Southern Ocean and Antarctica based on different proxies. Shaded bars indicate glacial intervals and the black numbers in the bars represent the marine isotope stages. (a) Alkenone U^{K}_{37}-derived sea surface temperature record at site GeoB 3327–5 in the Southeast Pacific. (b) Alkenone U^{K}_{37}-derived at site PS75/034–2 in the Southeast Pacific. (c) Alkenone-derived sea surface temperature records based on the $U^{K'}_{37}$ index (light purple curve) and the U^{K}_{37} index (dark purple curve) [*Martínez-Garcia et al.*, 2010; *Martínez-Garcia et al.*, 2009] at site PS2489–2/ODP Site 1090 in the South Atlantic. (d) Foraminiferal transfer function-derived summer SST record [*Becquey and Gersonde*, 2002, 2003] at site PS2489/ ODP Site 1090. The authors regarded the estimates for MIS 11 as an overestimation due to preferential dissolution of cold-water species. (e) Diatom transfer function-derived summer sea surface temperature record [*Schneider-Mor et al.*, 2008] at ODP Site 1093 in the South Atlantic. (f) Foraminiferal transfer function-derived winter SST record [*Schaefer et al.*, 2005] at site DSDP 594 in the Southwest Pacific. (g) Foraminiferal transfer function-derived winter SST record [*Howard and Prell*, 1992] at site E49–018 in the South Indian. (h) Atmospheric temperature record registered in the EPICA ice core at Dome C, Antarctica [*Jouzel et al.*, 2007].

deflected equatorward within the PCC instead of flowing through the Drake Passage as they do today, the transport to the South Atlantic would have been markedly reduced during glacials. In fact, such a scenario was invoked by *Gersonde et al.* [2003] to explain the intense cooling east of the Argentine basin during the LGM. The authors further hypothesized that such changes in the transport through the Drake Passage, which is one of the "Cold Water Routes" of the global thermohaline circulation, would have major implications for the global climate development. Our records corroborate their hypothesis and further suggest that the same mechanism might have occurred during all glacials prior to the LGM over the past 700 kyr.

5.4. Meridional SST Gradients: Equatorward Cold Water Transport

[34] Considering the large latitudinal range covered by the study sites, the alkenone-inferred SST records might be affected by different biogeographic patterns or seasonality. For instance, if the abundances of the alkenones or the source organisms (e.g., *E. huxleyi*) are skewed toward the warm/cold season at high/low latitudes [*Schneider et al.*, 2010], the resulting SST gradient would be artificially reduced. Thus our estimation of meridional SST gradients is conservative and might be underestimated.

[35] Our results show that in contrast to the pronounced glacial cooling in the subantarctic Pacific (~8°C), the amplitudes of glacial cooling decrease to ~4°C and ~1.5°C in the subtropics (GeoB 3388–1) and the tropics (HY04) (Figure 6), respectively. The glacial SST estimates in the subtropics (GeoB 3388–1) are 1°–2°C colder than the modern SST associated with the STF in the Southeast Pacific (~19°C), suggesting that the STF might have also shifted equatorward along with the SAF and the APF, albeit to a smaller extent, and resided slightly northward of our study site. The SST gradients between low and high latitudes (4°N at HY04 and 54°S at PS75/034–2) are steeper during glacials than interglacials, and the overall pattern resembles a mirror image of the high-latitude SST record (see Figure 6). The pattern holds even if other EEP SST records such as the ODP 846 (cold-tongue) and ODP 1239 (coastal upwelling) are used for gradient calculation. The more substantial glacial cooling at the higher latitudes leads to steeper SST gradients between the subantarctic and the subtropics than those between the subtropics and the tropics. Notably, the smaller tropical-subantarctic SST gradient during MIS 4 is of the same magnitude as those of MIS 8, 10, 12, 14, and 16, while the SST gradients are larger during MIS 2 and MIS 6. The finding of steeper SST gradients between the tropics and midlatitudes during glacials is consistent with the observation of *Kaiser et al.* [2005] over the past 70 kyr in the Southeast Pacific. However, their reconstruction suggested a slightly larger gradient (~1°C) during MIS 4 than during LGM, in contrast to ours. The discrepancy stems from the less intense cooling during MIS 4 at site GeoB 3388–1 relative to other glacials. Alternatively, it might also be due to a combination of other factors, including the lower temporal resolution in our records, records derived from different proxies (foraminiferal census count and Mg/Ca ratio) used in the gradient calculation of *Kaiser et al.* [2005], or different SST calibrations employed ($U^{K'}_{37}$ versus U^{K}_{37}). Notwithstanding, our records indicate that steeper meridional SST gradients during glacials are a recurring feature in the Southeast Pacific over the past 700 kyr.

[36] Several factors may contribute to the steeper high-to-low latitude gradients, including the insolation gradient and local hydrographic dynamics. The temporal resolution of our SST records is insufficient for determining the contribution of the local insolation gradient in shaping the meridional SST gradient, based on the wiggle-matching of the SST gradients to the insolation gradients (Figure 6). Besides, the subtropical site GeoB3388–1 might also be influenced by filaments advected from the coastal upwelling off Chile if the upwelling was stronger in the past. This notion, however, cannot be rigorously tested by our SST records and awaits future work based on more conservative water mass tracers. Alternatively, the steeper high-to-low latitude gradients during glacials might be linked to the vigor of the PCC. As readily observable in the modern day SST contour map (Figure 1), site GeoB 3388–1 is characterized by the advection of cold water from the south. It is conceivable that the steeper gradients between this site and the tropics (site HY 04 is beyond the influence of the east Pacific cold tongue) during the glacial periods are a result of enhanced cold water transport via an intensified PCC. Increased influence of ACC-sourced water in the subtropical Southeast Pacific has been inferred from enhanced glacial paleoproductivity, assuming that the main nutrient source was supplied from the south via the PCC [*Mohtadi and Hebbeln*, 2004; *Romero et al.*, 2006]. Increased transport by the PCC during glacials was invoked to explain the higher abundance of ACC cold-water coccolithophorid and dinoflagellate species at the midlatitudes Southeast Pacific [*Saavedra-Pellitero et al.*, 2011; *Verleye and Louwye*, 2010] and the increased cold-water foraminiferal abundance in the equatorial Pacific [*Feldberg and Mix*, 2002, 2003]. In addition, it has also been proposed on the basis of a steeper glacial meridional SST gradient at the equator, which suggested a northward shift of the Equator Front-Intertropical Convergence Zone (ITCZ) during glacial periods [*Rincón-Martínez et al.*, 2010]. Stronger cooling and intensification in the PCC transport (an eastern boundary current) during the glacial periods might have resulted from enhanced Ekman pumping from the subantarctic zone, as a response to an increase in wind strength and/or northward migration of the Westerlies. Such changes in the southern Westerlies have been inferred from some marine records [e.g., *Mohtadi and Hebbeln*, 2004; *Stuut and Lamy*, 2004]. Indeed, on the basis of the conservation of energy, a stronger zonal circulation north of the subantarctic zone could be deduced from steeper meridional gradients and an equatorward contraction of the subtropical realm. Moreover, as mentioned in section 5.3, an equatorward deflection of the major ACC fronts (the SAF and the APF) would also contribute to increased cold water transport via the PCC.

6. Conclusions

[37] The empirical relationship of U^{K}_{37}- and $U^{K'}_{37}$ with SST in our South Pacific regional core top data set is similar to

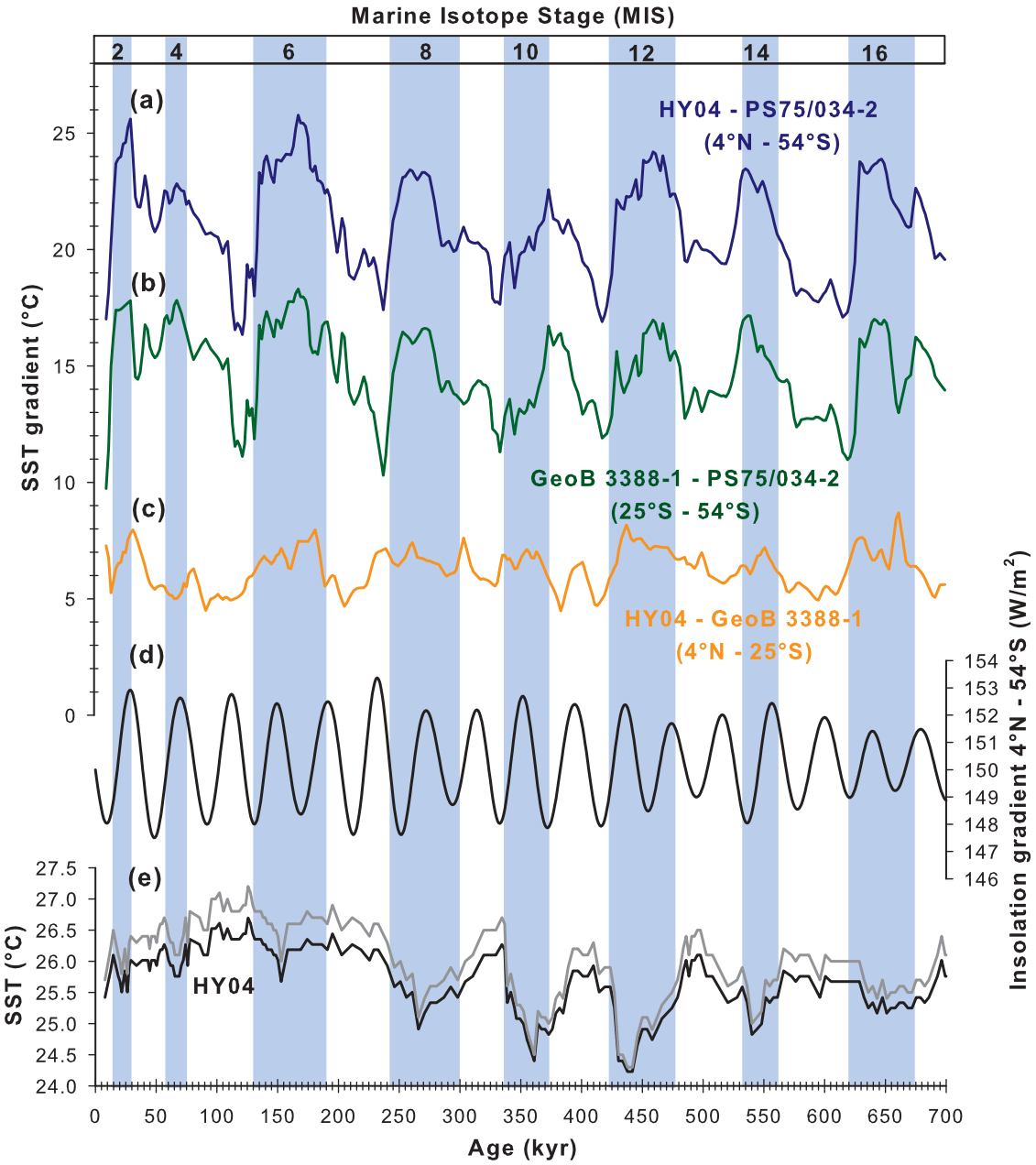

Figure 6. Meridional gradients of alkenone-inferred SSTs and mean annual insolation along the Southeast Pacific and SST evolution in the tropical Pacific. Shaded bars indicate glacial intervals, and the black numbers in the bars represent the marine isotope stages. The meridional SST gradients (a) between the tropics (HY04) and the subantarctic (PS75/034–2), (b) between the subtropics (GeoB 3388–1) and the subantartic (PS75/034–2), and (c) between the tropics (HY04) and the subtropics (GeoB 3388–1) are derived from U^{K}_{37} SST estimates calculated using the *E. huxleyi* culture calibration of *Prahl et al.* [1988]. (d) Meridional mean annual insolation gradient between 4°N and 54°S [*Laskar*, 1990]. (e) Alkenone-based SST records at site HY04 [*Horikawa et al.*, 2010]. For the SST gradient reconstruction, we recalculated the published SST using the U^{K}_{37} calibration of *Prahl et al.* [1988] (black curve) so that it is consistent with other SST records. The gray curve depicts the originally published SST record by *Horikawa et al.* [2010].

the commonly used calibrations derived from the laboratory *E. huxleyi* culture of *Prahl et al.* [1988]. These linear relationships hold even at low temperatures (down to ~1°C), suggesting that the temperature dependence of the alkenone indices is not lost at low temperatures in the Southern Ocean. This finding indicates that both alkenone indices are suitable for reconstructing SST at our cold subantarctic sites. However, these indices result in dissimilar SST patterns over the

past 700 kyr in the subantarctic Pacific. The $U^{K'}_{37}$-derived SST records display varying glacial severity, as opposed to the more uniform relative glacial/interglacial change in the U^{K}_{37}-inferred SST records. On the basis of the better agreement of the glacial severity patterns of the U^{K}_{37} records with that of the planktic $\delta^{18}O$ at the same sites and other subantarctic SST records, we conclude that the U^{K}_{37} is a more suitable index for paleo SST reconstruction in the subantarctic Pacific. The U^{K}_{37}-derived SST records suggest pronounced glacial cooling of ~8°C and ~4°C in the subantarctic and the subtropical regions, respectively. The magnitude of subantarctic glacial cooling is comparable to that reported for other sectors of the Southern Ocean. The SST estimates also suggest that the ACC and its associated fronts migrated equatorward by 7° to 9° during glacials over the past 700 kyr, which might have reduced the water transport through the Drake Passage to the South Atlantic. Conversely, the deflection of more ACC waters equatorward during glacials probably enhanced the cold water advection via the PCC, resulting in colder subtropical SSTs and thus larger meridional SST gradients between the tropics and the subtropics.

[38] **Acknowledgments.** Constructive comments from three anonymous reviewers and the Editor, Rainer Zahn, have improved the manuscript tremendously. We are grateful to Giuseppe Cortese for sharing his unpublished data. Thanks also go to Gemma Rueda, Susanne Fietz, Nicole Meyer, and Hendrik Grotheer for assisting in the alkenone analysis. Technical support from Walter Luttmer and Ralph Kreutz in the laboratories is also highly appreciated. We acknowledge the POLMAR Graduate School for funding S.L.H's Ph.D. study at the Alfred Wegener Institute and a SCAR Fellowship 2010/2011 for funding S.L.H's short stay at the Autonomous University of Barcelona during the preparation of PS75 core top samples.

References

Bard, E. (2001), Comparison of alkenone estimates with other paleotemperature proxies, *Geochem. Geophys. Geosyst.*, *2*(1), 1002, doi:10.1029/2000GC000050.

Bard, E., and R. E. M. Rickaby (2009), Migration of the subtropical front as a modulator of glacial climate, *Nature*, *460*(7253), 380–383, doi:10.1038/nature08189.

Barrows, T. T., and S. Juggins (2005), Sea-surface temperatures around the Australian margin and Indian Ocean during the Last Glacial Maximum, *Quat. Sci. Rev.*, *24*(7–9), 1017–1047, doi:10.1016/j.quascirev.2004.07.020.

Becquey, S., and R. Gersonde (2002), Past hydrographic and climatic changes in the Subantarctic Zone of the South Atlantic-The Pleistocene record from ODP Site 1090, *Palaeogeogr. Palaeoclimatol. Palaeoecol.*, *182*(3–4), 221–239, doi:10.1016/S0031-0182(01)00497-7.

Becquey, S., and R. Gersonde (2003), A 0.55-Ma paleotemperature record from the Subantarctic zone: Implications for Antarctic Circumpolar Current development, *Paleoceanography*, *18*(1), 1014, doi:10.1029/2000PA000576.

Bendle, J., and A. Rosell-Melé (2004), Distributions of U^{K}_{37} and $U^{K'}_{37}$ in the surface waters and sediments of the Nordic Seas: Implications for paleoceanography, *Geochem. Geophys. Geosyst.*, *5*, Q11013, doi:10.1029/2004GC000741.

Bendle, J., A. Rosell-Melé, and P. Ziveri (2005), Variability of unusual distributions of alkenones in the surface waters of the Nordic seas, *Paleoceanography*, *20*, PA2001, doi:10.1029/2004PA001025.

Brassell, S. C., G. Eglinton, I. T. Marlowe, U. Pflaumann, and M. Sarnthein (1986), Molecular stratigraphy - a new tool for climatic assessment, *Nature*, *320*(6058), 129–133, doi:10.1038/320129a0.

Caniupán, M., et al. (2011), Millennial-scale sea surface temperature and Patagonian Ice Sheet changes off southernmost Chile (53°S) over the past 60 kyr, *Paleoceanography*, *26*, PA3221, doi:10.1029/2010PA002049.

Chaigneau, A., and O. Pizarro (2005), Surface circulation and fronts of the South Pacific Ocean, east of 120°W, *Geophys. Res. Lett.*, *32*, L08605, doi:10.1029/2004GL022070.

Conte, M. H., M. A. Sicre, C. Ruhlemann, J. C. Weber, S. Schulte, D. Schulz-Bull, and T. Blanz (2006), Global temperature calibration of the alkenone unsaturation index ($U^{K'}_{37}$) in surface waters and comparison with surface sediments, *Geochem. Geophys. Geosyst.*, *7*, Q02005, doi:10.1029/2005GC001054.

Crosta, X., A. Sturm, L. Armand, and J.-J. Pichon (2004), Late Quaternary sea ice history in the Indian sector of the Southern Ocean as recorded by diatom assemblages, *Mar. Micropaleontol.*, *50*(3–4), 209–223, doi:10.1016/S0377-8398(03)00072-0.

Cunningham, S. A., S. G. Alderson, B. A. King, and M. A. Brandon (2003), Transport and variability of the Antarctic Circumpolar Current in Drake Passage, *J. Geophys. Res.*, *108*(C5), 8084, doi:10.1029/2001JC001147.

de Vernal, A., A. Rosell-Melé, M. Kucera, C. Hillaire-Marcel, F. Eynaud, M. Weinelt, T. Dokken, and M. Kageyama (2006), Comparing proxies for the reconstruction of LGM sea-surface conditions in the northern North Atlantic, *Quat. Sci. Rev.*, *25*(21–22), 2820–2834, doi:10.1016/j.quascirev.2006.06.006.

Feldberg, M. J., and A. C. Mix (2002), Sea-surface temperature estimates in the Southeast Pacific based on planktonic foraminiferal species; modern calibration and Last Glacial Maximum, *Mar. Micropaleontol.*, *44*(1–2), 1–29, doi:10.1016/S0377-8398(01)00035-4.

Feldberg, M. J., and A. C. Mix (2003), Planktonic foraminifera, sea surface temperatures, and mechanisms of oceanic change in the Peru and south equatorial currents, 0–150 ka BP, *Paleoceanography*, *18*(1), 1016, doi:10.1029/2001PA000740.

Fietz, S., A. Martinez-Garcia, G. Rueda, V. L. Peck, C. Huguet, M. Escala, and A. Rosell-Melé (2011), Crenarchaea and phytoplankton coupling in sedimentary archives: Common trigger or metabolic dependence?, *Limnol. Oceanogr.*, *56*(5), 1907–1916, doi:10.4319/lo.2011.56.5.1907.

Fischer, H., et al. (2010), The role of Southern Ocean processes in orbital and millennial CO_2 variations–A synthesis, *Quat. Sci. Rev.*, *29*(1–2), 193–205, doi:10.1016/j.quascirev.2009.06.007.

Gersonde, R., et al. (2003), Last glacial sea surface temperatures and sea-ice extent in the Southern Ocean (Atlantic-Indian sector): A multiproxy approach, *Paleoceanography*, *18*(3), 1061, doi:10.1029/2002PA000809.

Gersonde, R., X. Crosta, A. Abelmann, and L. Armand (2005), Sea-surface temperature and sea ice distribution of the Southern Ocean at the EPILOG Last Glacial Maximum - A circum-Antarctic view based on siliceous microfossil records, *Quat. Sci. Rev.*, *24*(7–9), 869–896, doi:10.1016/j.quascirev.2004.07.015.

Gersonde, R., et al. (2011), The expedition of the research vessel "Polarstern" to the polar South Pacific in 2009/2010(ANT-XXVI/2 - BIPOMAC), *Rep. Polar Marine Res.*, *632*, 1–330.

Harada, N., N. Ahagon, T. Sakamoto, M. Uchida, M. Ikehara, and Y. Shibata (2006), Rapid fluctuation of alkenone temperature in the southwestern Okhotsk Sea during the past 120 ky, *Global Planet. Change*, *53*(1–2), 29–46, doi:10.1016/j.gloplacha.2006.01.010.

Hays, J. D., J. Imbrie, and N. J. Shackleton (1976), Variations in the earth's orbit: Pacemaker of the ice ages, *Science*, *194*(4270), 1121–1132, doi:10.1126/science.194.4270.1121.

Hebbeln, D., G. Wefer, and C. Participants (1995), Cruise report of R/V Sonne cruise 102, report, 166 pp., Univ. of Bremen, Germany.

Horikawa, K., M. Murayama, M. Minagawa, Y. Kato, and T. Sagawa (2010), Latitudinal and downcore (0–750 ka) changes in n-alkane chain lengths in the eastern equatorial Pacific, *Quat. Res.*, *73*(3), 573–582, doi:10.1016/j.yqres.2010.01.001.

Howard, W. R., and W. L. Prell (1992), Late quaternary surface circulation of the southern Indian Ocean and its relationship to orbital variations, *Paleoceanography*, *7*(1), 79–117, doi:10.1029/91PA02994.

Jouzel, J., et al. (2007), Orbital and millennial Antarctic climate variability over the past 800,000 years, *Science*, *317*(5839), 793–796, doi:10.1126/science.1141038.

Kaiser, J., F. Lamy, and D. Hebbeln (2005), A 70-kyr sea surface temperature record off southern Chile (Ocean Drilling Program Site 1233), *Paleoceanography*, *20*, PA4009, doi:10.1029/2005PA001146.

Kidston, J., A. S. Tashetto, D. W. J. Thompson, and M. H. England (2011), The influence of Southern Hemisphere sea-ice extent on the latitude of the mid-latitude jet stream, *Geophys. Res. Lett.*, *38*, L15804, doi:10.1029/2011GL048056.

Kienast, M., G. MacIntyre, N. Dubois, S. Higginson, C. Normandeau, C. Chazen, and T. D. Herbert (2012), Alkenone unsaturation in surface sediments from the eastern equatorial Pacific: Implications for SST reconstructions, *Paleoceanography*, *27*, PA1210, doi:10.1029/2011PA002254.

Lamy, F., J. Kaiser, U. Ninnemann, D. Hebbeln, H. W. Arz, and J. Stoner (2004), Antarctic timing of surface water changes off Chile and Patagonian ice sheet response, *Science*, *304*(5679), 1959–1962, doi:10.1126/science.1097863.

Lang, N., and E. W. Wolff (2011), Interglacial and glacial variability from the last 800 ka in marine, ice and terrestrial archives, *Clim. Past*, *7*(2), 361–380, doi:10.5194/cp-7-361-2011.

Laskar, J. (1990), The chaotic motion of the solar system: A numerical estimate of the size of the chaotic zones, *Icarus*, *88*(2), 266–291, doi:10.1016/0019-1035(90)90084-M.

Lisiecki, L. E., and M. E. Raymo (2005), A Pliocene-Pleistocene stack of 57 globally distributed benthic δO^{18} records, *Paleoceanography*, *20*, PA1003, doi:10.1029/2004PA001071.

Luz, B. (1977), Late Pleistocene paleoclimates of the South Pacific based on statistical analysis of planktonic foraminifers, *Palaeogeogr. Palaeoclimatol. Palaeoecol.*, *22*(1), 61–78, doi:10.1016/0031-0182(77)90033-5.

Marshall, J., and K. Speer (2012), Closure of the meridional overturning circulation through Southern Ocean upwelling, *Nat. Geosci.*, *5*(3), 171–180, doi:10.1038/ngeo1391.

Martínez-Garcia, A., A. Rosell-Melé, W. Geibert, R. Gersonde, P. Masque, V. Gaspari, and C. Barbante (2009), Links between iron supply, marine productivity, sea surface temperature, and CO_2 over the last 1.1 Ma, *Paleoceanography*, *24*, PA1207, doi:10.1029/2008PA001657.

Martínez-Garcia, A., A. Rosell-Melé, E. L. McClymont, R. Gersonde, and G. H. Haug (2010), Subpolar link to the emergence of the modern equatorial Pacific cold tongue, *Science*, *328*(5985), 1550–1553, doi:10.1126/science.1184480.

Mohtadi, M., and D. Hebbeln (2004), Mechanisms and variations of the paleoproductivity off northern Chile (24°S & 33°S) during the last 40,000 years, *Paleoceanography*, *19*, PA2023, doi:10.1029/2004PA001003.

Mohtadi, M., D. Hebbeln, S. Nuñez Ricardo, and C. B. Lange (2006), El Niño-like pattern in the Pacific during marine isotope stages (MIS) 13 and 11?, *Paleoceanography*, *21*, PA1015, doi:10.1029/2005PA001190.

Müller, P. J., G. Kirst, G. Ruhland, I. von Storch, and A. Rosell-Melé (1998), Calibration of the alkenone paleotemperature index $U^{K'}_{37}$ based on core-tops from the eastern South Atlantic and the global ocean (60°N–60°S), *Geochim. Cosmochim. Acta*, *62*(10), 1757–1772, doi:10.1016/S0016-7037(98)00097-0.

Orsi, A. H., T. Whitworth, and W. D. Nowlin (1995), On the meridional extent and fronts of the Antarctic Circumpolar Current, *Deep Sea Res., Part I*, *42*(5), 641–673, doi:10.1016/0967-0637(95)00021-W.

Pahnke, K., R. Zahn, H. Elderfield, and M. Schulz (2003), 340,000-year centennial-scale marine record of Southern Hemisphere climatic oscillation, *Science*, *301*(5635), 948–952, doi:10.1126/science.1084451.

Paillard, D., L. Labeyrie, and P. Yiou (1996), Macintosh program performs time-series analysis, *Eos Trans. AGU*, *77*(39), 379, doi:10.1029/96EO00259.

Parrenin, F., et al. (2007), The EDC3 chronology for the EPICA dome C ice core, *Clim. Past*, *3*(3), 485–497, doi:10.5194/cp-3-485-2007.

Petit, J. R., et al. (1999), Climate and atmospheric history of the past 420,000 years from the Vostok ice core, Antarctica, *Nature*, *399*(6735), 429–436, doi:10.1038/20859.

Prahl, F. G., and S. G. Wakeham (1987), Calibration of unsaturation patterns in long-chain ketone compositions for paleotemperature assessment, *Nature*, *330*(6146), 367–369, doi:10.1038/330367a0.

Prahl, F. G., L. A. Muehlhausen, and D. L. Zahnle (1988), Further evaluation of long-chain alkenones as indicators of paleoceanographic conditions, *Geochim. Cosmochim. Acta*, *52*(9), 2303–2310, doi:10.1016/0016-7037(88)90132-9.

Rincón-Martínez, D., F. Lamy, S. Contreras, G. Leduc, E. Bard, C. Saukel, T. Blanz, A. Mackensen, and R. Tiedemann (2010), More humid interglacials in Ecuador during the past 500 kyr linked to latitudinal shifts of the equatorial front and the Intertropical Convergence Zone in the eastern tropical Pacific, *Paleoceanography*, *25*, PA2210, doi:10.1029/2009PA001868.

Romero, O. E., J.-H. Kim, and D. Hebbeln (2006), Paleoproductivity evolution off central Chile from the Last Glacial Maximum to the Early Holocene, *Quat. Res.*, *65*(3), 519–525, doi:10.1016/j.yqres.2005.07.003.

Rosell-Melé, A. (1998), Interhemispheric appraisal of the value of alkenone indices as temperature and salinity proxies in high-latitude locations, *Paleoceanography*, *13*(6), 694–703, doi:10.1029/98PA02355.

Rosell-Melé, A., and P. Comes (1999), Evidence for a warm Last Glacial Maximum in the Nordic seas or an example of shortcomings in $U^{K'}_{37}$ and U^{K}_{37} to estimate low sea surface temperature?, *Paleoceanography*, *14*(6), 770–776, doi:10.1029/1999PA900037.

Rosell-Melé, A., J. Carter, and G. Eglinton (1994), Distributions of long-chain alkenones and alkyl alkenoates in marine surface sediments from the North East Atlantic, *Org. Geochem.*, *22*(3–5), 501–509, doi:10.1016/0146-6380(94)90122-8.

Rosell-Melé, A., G. Eglinton, U. Pflaumann, and M. Sarnthein (1995), Atlantic core-top calibration of the U^{K}_{37} index as a sea-surface palaeotemperature indicator, *Geochim. Cosmochim. Acta*, *59*(15), 3099–3107, doi:10.1016/0016-7037(95)00199-A.

Saavedra-Pellitero, M., J. A. Flores, F. Lamy, F. J. Sierro, and A. Cortina (2011), Coccolithophore estimates of paleotemperature and paleoproductivity changes in the southeast Pacific over the past 27 kyr, *Paleoceanography*, *26*, PA1201, doi:10.1029/2009PA001824.

Schaefer, G., J. S. Rodger, B. W. Hayward, J. P. Kennett, A. T. Sabaa, and G. H. Scott (2005), Planktic foraminiferal and sea surface temperature record during the last 1 Myr across the Subtropical Front, Southwest Pacific, *Mar. Micropaleontol.*, *54*(3–4), 191–212, doi:10.1016/j.marmicro.2004.12.001.

Schneider, B., G. Leduc, and W. Park (2010), Disentangling seasonal signals in Holocene climate trends by satellite-model-proxy integration, *Paleoceanography*, *25*, PA4217, doi:10.1029/2009PA001893.

Schneider, R. R., P. J. Müller, and R. Acheson (1999), Atlantic alkenone sea-surface temperature records: Low versus mid latitudes and differences between hemispheres, in *Reconstructing Ocean History: A Window into the Future*, edited by F. Abrantes and A. C. Mix, pp. 33–55, Kluwer Acad., New York.

Schneider-Mor, A., R. Yam, C. Bianchi, M. Kunz-Pirrung, R. Gersonde, and A. Shemesh (2008), Nutrient regime at the siliceous belt of the Atlantic sector of the Southern Ocean during the past 660 ka, *Paleoceanography*, *23*, PA3217, doi:10.1029/2007PA001466.

Shackleton, N. J. (1987), Oxygen isotopes, ice volume and sea level, *Quat. Sci. Rev.*, *6*(3–4), 183–190, doi:10.1016/0277-3791(87)90003-5.

Shackleton, N. J., A. Berger, and W. R. Peltier (1990), An alternative astronomical calibration of the lower Pleistocene timescale based on ODP Site 677, *Trans. R. Soc. Edinburgh Earth Sci.*, *81*(04), 251–261, doi:10.1017/S0263593300020782.

Sikes, E. L., and J. K. Volkman (1993), Calibration of alkenone unsaturation ratios ($U^{k'}_{37}$) for paleotemperature estimation in cold polar waters, *Geochim. Cosmochim. Acta*, *57*(8), 1883–1889, doi:10.1016/0016-7037(93)90120-L.

Sikes, E. L., J. K. Volkman, L. G. Robertson, and J. J. Pichon (1997), Alkenones and alkenes in surface waters and sediments of the Southern Ocean: Implications for paleotemperature estimation in polar regions, *Geochim. Cosmochim. Acta*, *61*, 1495–1505, doi:10.1016/S0016-7037(97)00017-3.

Sonzogni, C., E. Bard, F. Rostek, R. Lafont, A. Rosell-Mele, and G. Eglinton (1997), Core-top calibration of the alkenone index vs sea surface temperature in the Indian Ocean, *Deep Sea Res., Part II*, *44*(6–7), 1445–1460, doi:10.1016/S0967-0645(97)00010-6.

Strub, P. T., J. M. Mesias, V. Montecino, J. Rutlant, and S. Salinas (1998), *Coastal Ocean Circulation Off Western South America*, John Wiley, New York.

Stuut, J.-B. W., and F. Lamy (2004), Climate variability at the southern boundaries of the Namib (southwestern Africa) and Atacama (northern Chile) coastal deserts during the last 120,000 yr, *Quat. Res.*, *62*(3), 301–309, doi:10.1016/j.yqres.2004.08.001.

Venz, K. A., and D. A. Hodell (2002), New evidence for changes in Plio-Pleistocene deep water circulation from Southern Ocean ODP Leg 177 Site 1090, *Palaeogeogr. Palaeoclimatol. Palaeoecol.*, *182*, 197–220, doi:10.1016/S0031-0182(01)00496-5.

Verleye, T. J., and S. Louwye (2010), Late Quaternary environmental changes and latitudinal shifts of the Antarctic Circumpolar Current as recorded by dinoflagellate cysts from offshore Chile (41°S), *Quat. Sci. Rev.*, *29*(7–8), 1025–1039, doi:10.1016/j.quascirev.2010.01.009.

Villanueva, J., and J. O. Grimalt (1996), Pitfalls in the chromatographic determination of the alkenone U^{k}_{37} index for paleotemperature estimation, *J. Chromatogr. A*, *723*(2), 285–291, doi:10.1016/0021-9673(95)00471-8.

Wells, P., and H. Okada (1997), Response of nannoplankton to major changes in sea-surface temperature and movements of hydrological fronts over Site DSDP 594(south Chatham Rise, southeastern New Zealand), during the last 130 kyr, *Mar. Micropaleontol.*, *32*(3–4), 341–363, doi:10.1016/S0377-8398(97)00025-X.

Wyrtki, K. (1965), Oceanography of the eastern equatorial Pacific Ocean, *Oceanogr. Mar. Biol.*, *4*, 33–68.

Zielinski, U., and R. Gersonde (2002), Plio–Pleistocene diatom biostratigraphy from ODP Leg 177, Atlantic sector of the Southern Ocean, *Mar. Micropaleontol.*, *45*(3–4), 225–268, doi:10.1016/S0377-8398(02)00031-2.